

Structure of Pb²⁺/deprotonated dGMP complexes in the gas phase: A combined MS-MS/IRMPD spectroscopy/ion mobility study.

*Jean-Yves Salpin^{*1,2}, Luke MacAleese^{*3,4}, Fabien Chiro^{5,6}, Philippe Dugourd^{3,4},*

1) Université d'Evry Val d'Essonne – Laboratoire Analyse et Modélisation pour la Biologie et l'Environnement – Boulevard François Mitterrand – 91025 Evry – France
2) CNRS- UMR 8587.

3) Université Lyon 1– Institut Lumière Matière, 5 rue de la Doua, 69622 Villeurbanne cedex – France

4) CNRS- UMR 5306.

5) Université Lyon 1 – Institut des Sciences Analytiques, 5 rue de la Doua, 69100 Villeurbanne – France

6) CNRS- UMR 5280

Supporting information

1S. Low-energy CID spectrum of the [Pb(GMP)-H]⁺ complex recorded at 30 eV (laboratory frame).

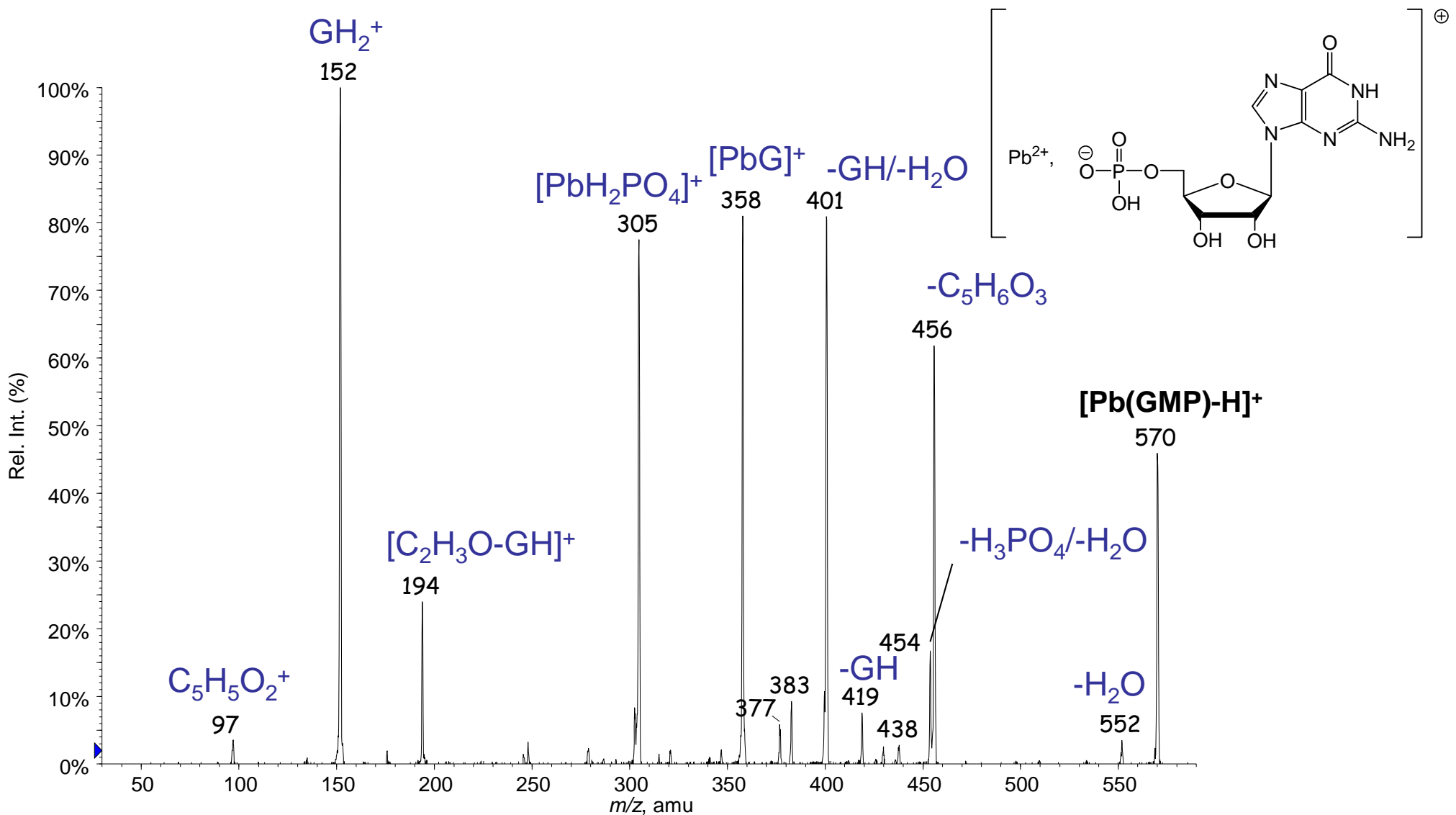
2S. Structure and geometrical details of the various structures optimized for the [Pb(dGMP)-H]⁺ complex

3S. Total energy and ZPE (Hartree) of the various structures considered

4S. DFT-computed IR absorption spectra for the [Pb(dGMP)-H]⁺ structures. The experimental IRMPD spectrum is overlayed in grey.

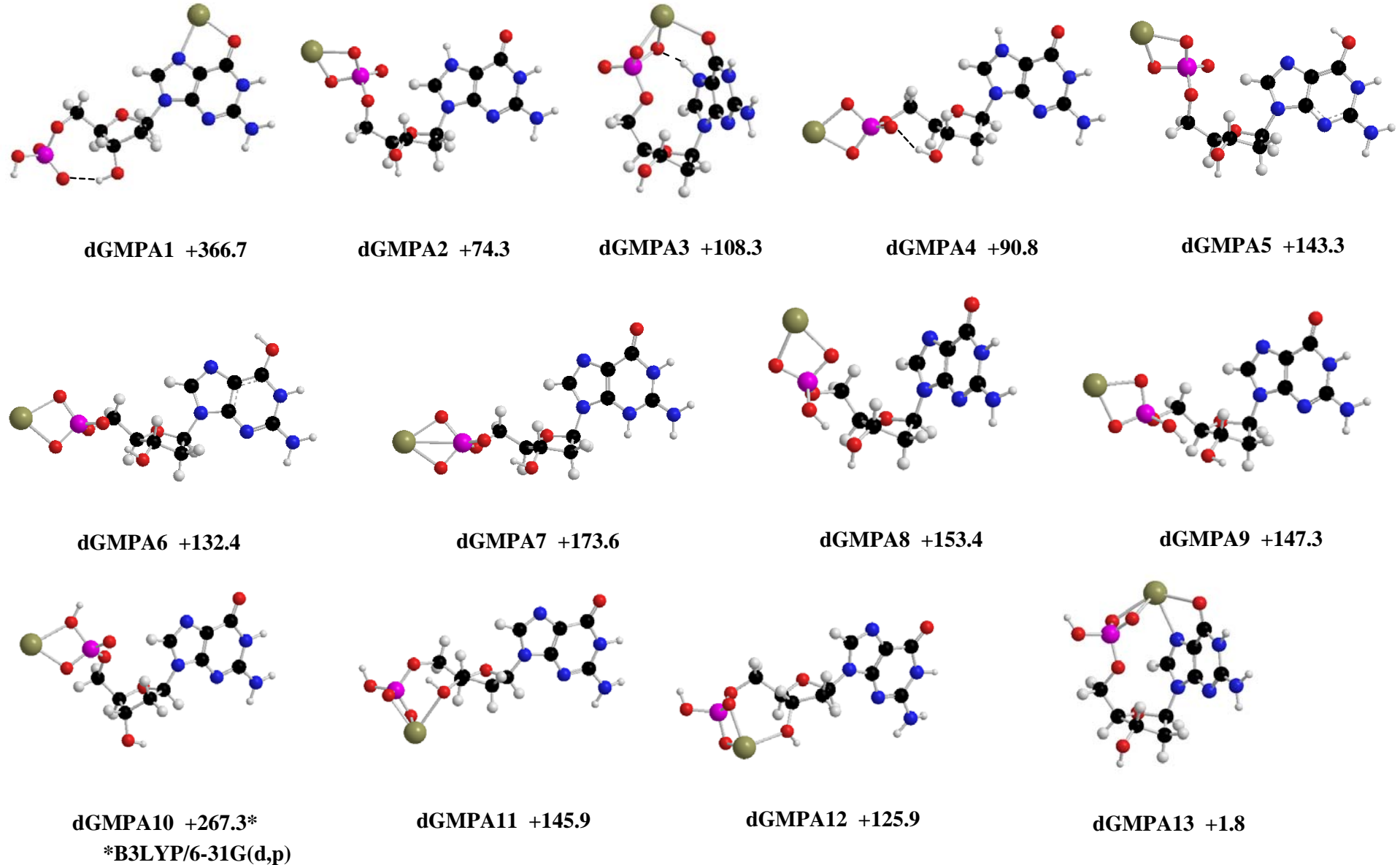
5S. Evolution of [Pb(dGMP)-H]⁺ arrival time as a function of 1/E, the electric field applied across the mobility tube.

1S. Low-energy CID spectrum of the $[\text{Pb}(\text{GMP})\text{-H}]^+$ complex recorded at 30 eV (laboratory frame).

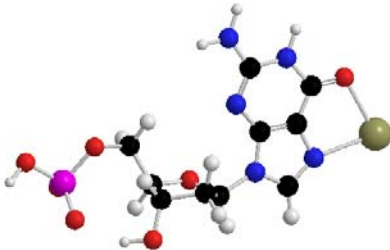


2S. Structure and geometrical details of the various structures optimized for the $[\text{Pb}(\text{dGMP})\text{-H}]^+$ complex. Relative free energies determined at the B3LYP/6-31++G(2df,2p)//B3LYP/6-31G(d,p) level

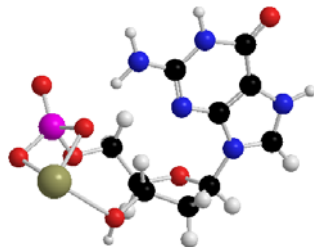
2.1 Anti forms



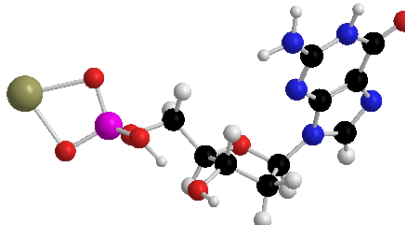
2.2 Syn forms



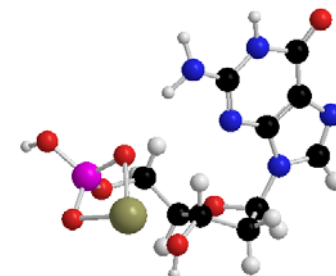
dGMPS1 +383.0*
* B3LYP/6-31G(d,p)



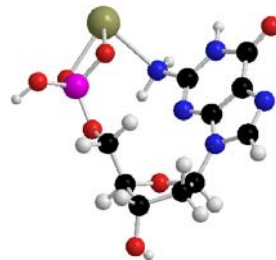
dGMPS2 +119.6



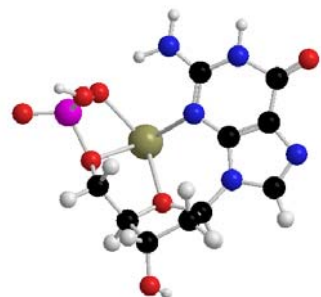
dGMPS3 +144.4



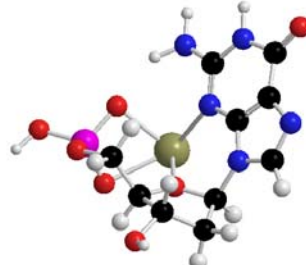
dGMPS4 +126.4



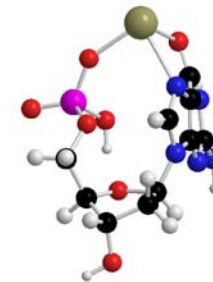
dGMPS5 +161.5



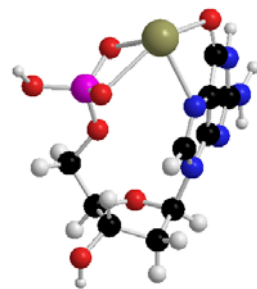
dGMPS6 +130.8



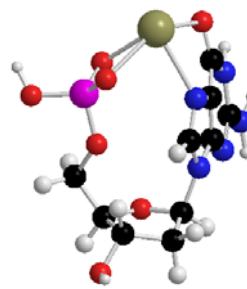
dGMPS7 +85.0



dGMPS8 +74.8



dGMPS9 +9.5



dGMPS10 0.0

2.3 Summary

Structures	Interaction sites								Sugar conformation ^(a)	Intramolecular H bonds
	Phosphate	O4'	OH 3'	OH 5'	C=O (6)	NH ₂	N1	N3	N7	
<i>Anti forms^(b)</i>										
dGMPA1					○				○	C2'-endo/C1'-exo (² T ₁)
dGMPA2	○ (O ⁻ /O ⁻)									C3'-endo/C2'-exo (³ T ₂)
dGMPA3	○ (O ⁻ /O ⁻)				○					C3'-endo/C2'-exo (³ T ₂)
dGMPA4	○ (O ⁻ /O ⁻)									C3'-endo (³ E)
dGMPA5	○ (O ⁻ /O ⁻)									C3'-endo/C2'-exo (³ T ₂)
dGMPA6	○ (O ⁻ /O ⁻)									C3'-endo (³ E)
dGMPA7	○ (O ⁻ /O ⁻)									C3'-endo/C2'-exo (³ T ₂)
dGMPA8	○ (=O/O ⁻)									C3'-endo/C2'-exo (³ T ₂)
dGMPA9	○ (=O/O ⁻)									C3'-endo/C2'-exo (³ T ₂)
dGMPA10	○ (O ⁻ /OH)									C2'-endo/C3'-exo (² T ₃)
dGMPA11	○ (=O/O ⁻)		○							C3'-endo/C4'-exo (³ T ₄)
dGMPA12	○ (=O/O ⁻)		○							O4'-endo/C1'-exo (⁰ T ₁)
dGMPA13	○ (=O/O ⁻)				○				○	C3'-endo/C2'-exo (³ T ₂)
<i>Syn forms^(b)</i>										
dGMPS1					○				○	C2'-endo/C1'-exo (² T ₁)
dGMPS2	○ (O ⁻ /O ⁻)		○							C3'-endo/C2'-exo (³ T ₂)
dGMPS3	○ (=O/O ⁻)									C3'-endo/C2'-exo (³ T ₂)
dGMPS4	○ (=O/O ⁻)		○							C3'-endo/C2'-exo (³ T ₂)
dGMPS5	○ (=O/O ⁻)					○				C2'-endo/C3'-exo (² T ₃)
dGMPS6	○ (O ⁻)	○		○				○		C2'-endo/C3'-exo (² T ₃)
dGMPS7	○ (=O/O ⁻)	○						○		C3'-endo/C2'-exo (³ T ₂)
dGMPS8	○ (O ⁻)				○			○		C2'-endo/C3'-exo (² T ₃)
dGMPS9	○ (=O/O ⁻)				○			○		C3'-endo/C2'-exo (³ T ₂)
dGMPS10	○ (=O/O ⁻)				○				○	C3'-endo/C2'-exo (³ T ₂)

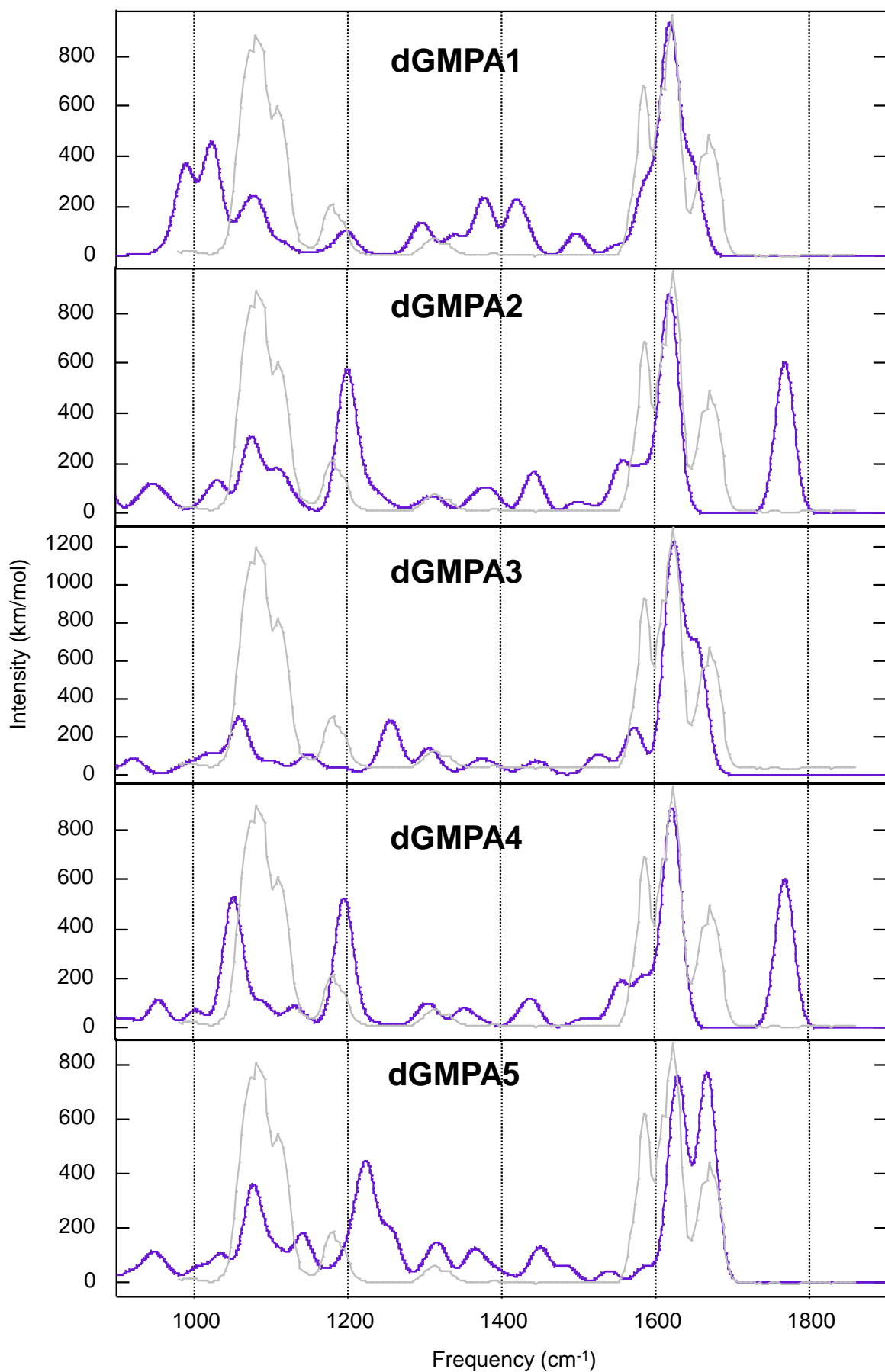
(a) Four ring atoms are considered as planar (E forms) when their associated torsional angle is greater than 179°

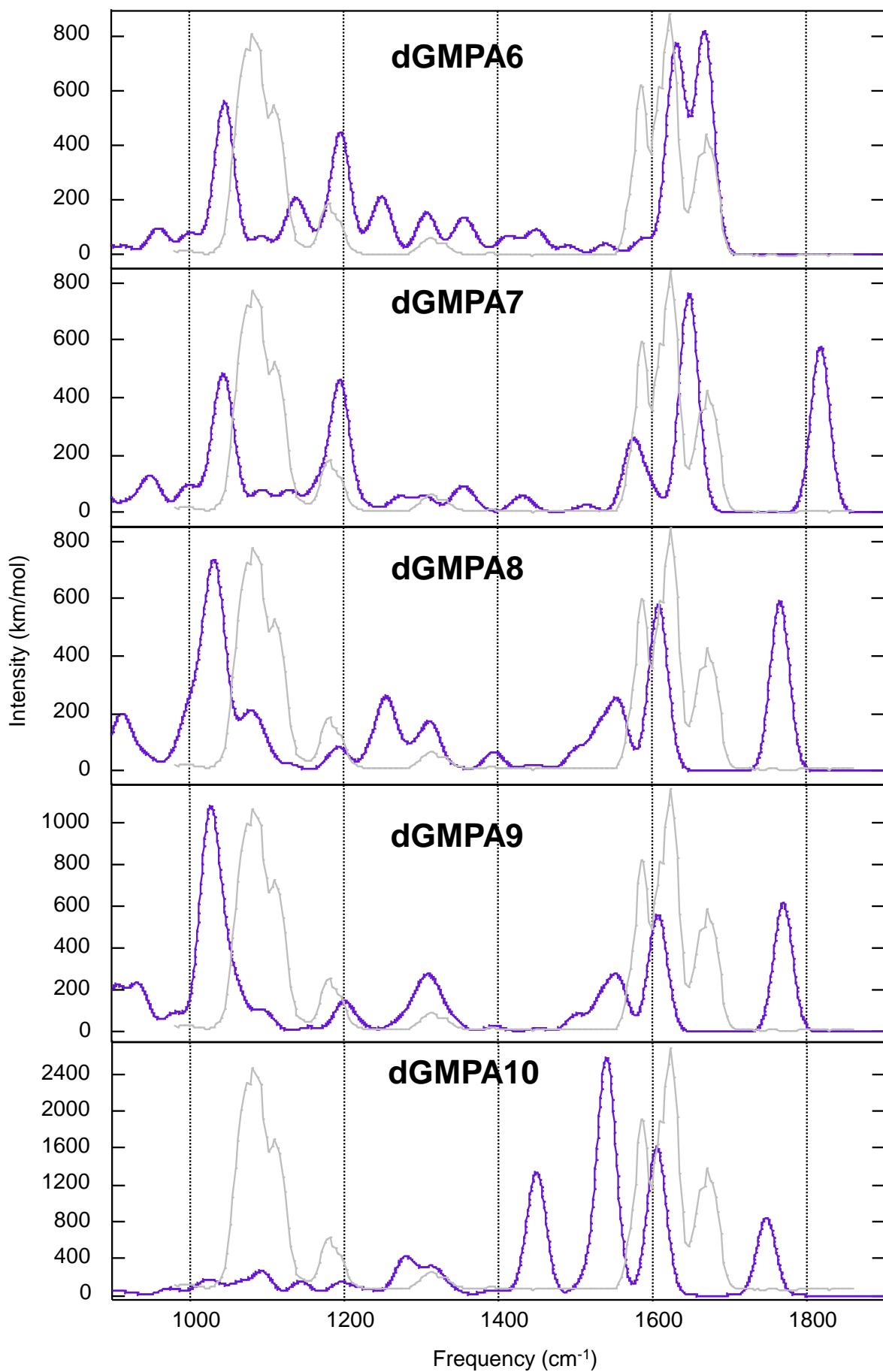
(b) By convention, the *Syn* conformation (S) corresponds to a C4-N9-C'1-O4' torsional angle ranging from 0 to ±90°. Otherwise, the conformation is *Anti* (A)

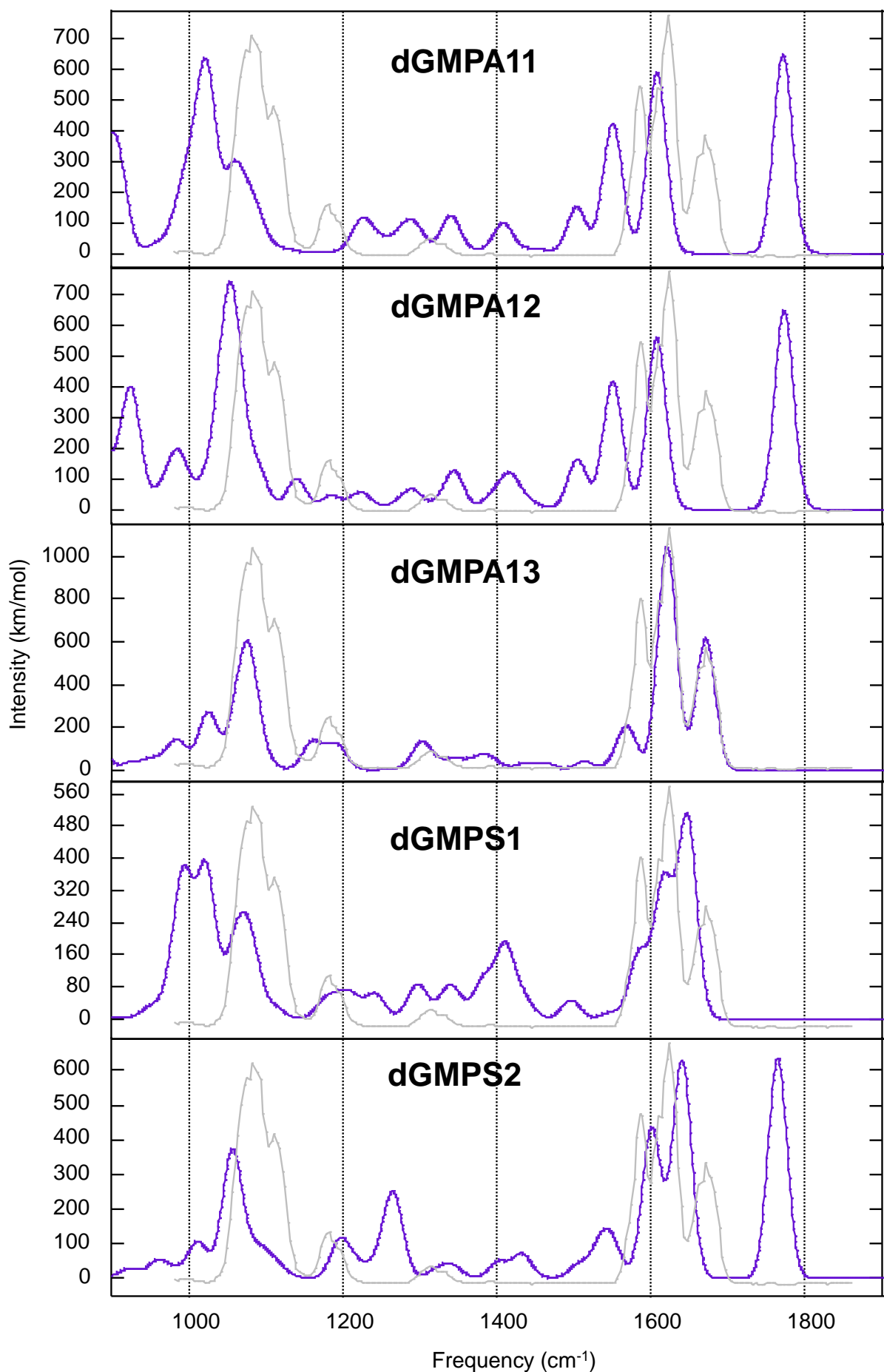
3S. Total energy, thermal correction to Gibbs free energy (TCG) and ZPE (Hartree) of the various structures considered during this study.

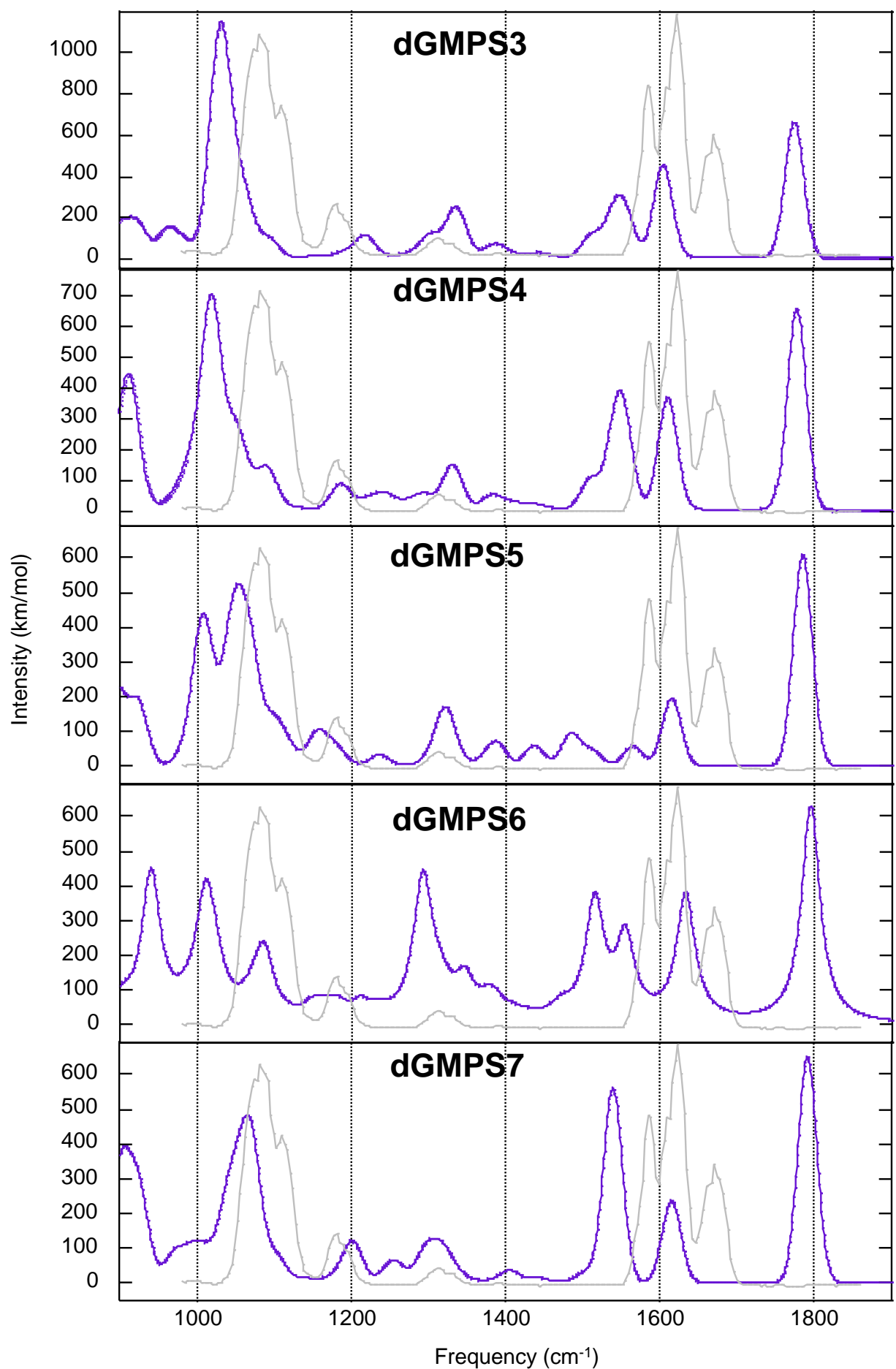
Structure	B3LYP/6-31G(d,p)			B3LYP//6-311+G(2df,2p)
	E	ZPE	TCG	E
dGMPA1	-1533.845199	0.266534	0.209900	-1534.329415
dGMPA2	-1533.956524	0.268431	0.212373	-1534.443255
dGMPA3	-1533.955654	0.267647	0.216837	-1534.434760
dGMPA4	-1533.951044	0.269049	0.212966	-1534.437542
dGMPA5	-1533.930100	0.268004	0.211968	-1534.41654
dGMPA6	-1533.93549	0.268700	0.212493	-1534.421218
dGMPA7	-1533.917473	0.267758	0.211300	-1534.404346
dGMPA8	-1533.928523	0.268243	0.213293	-1534.414012
dGMPA9	-1533.928081	0.267856	0.211509	-1534.414562
dGMPA10	-1533.881039	0.265704	0.206523	
dGMPA11	-1533.929477	0.266978	0.211334	-1534.414943
dGMPA12	-1533.93568	0.266842	0.211183	-1534.422404
dGMPA13	-1533.993128	0.268303	0.216814	-1534.475306
dGMPS1	-1533.841038	0.266733	0.210618	
dGMPS2	-1533.951487	0.269717	0.218234	-1534.431864
dGMPS3	-1533.929210	0.267705	0.212417	-1534.416566
dGMPS4	-1533.942752	0.267361	0.214402	-1534.425433
dGMPS5	-1533.928814	0.267843	0.214730	-1534.412366
dGMPS6	-1533.945020	0.267200	0.214716	-1534.424076
dGMPS7	-1533.961591	0.267712	0.215996	-1534.442794
dGMPS8	-1533.965819	0.268626	0.217449	-1534.448121
dGMPS9	-1533.987905	0.268021	0.215972	-1534.471506
dGMPS10	-1533.989783	0.267613	0.215146	-1534.474311

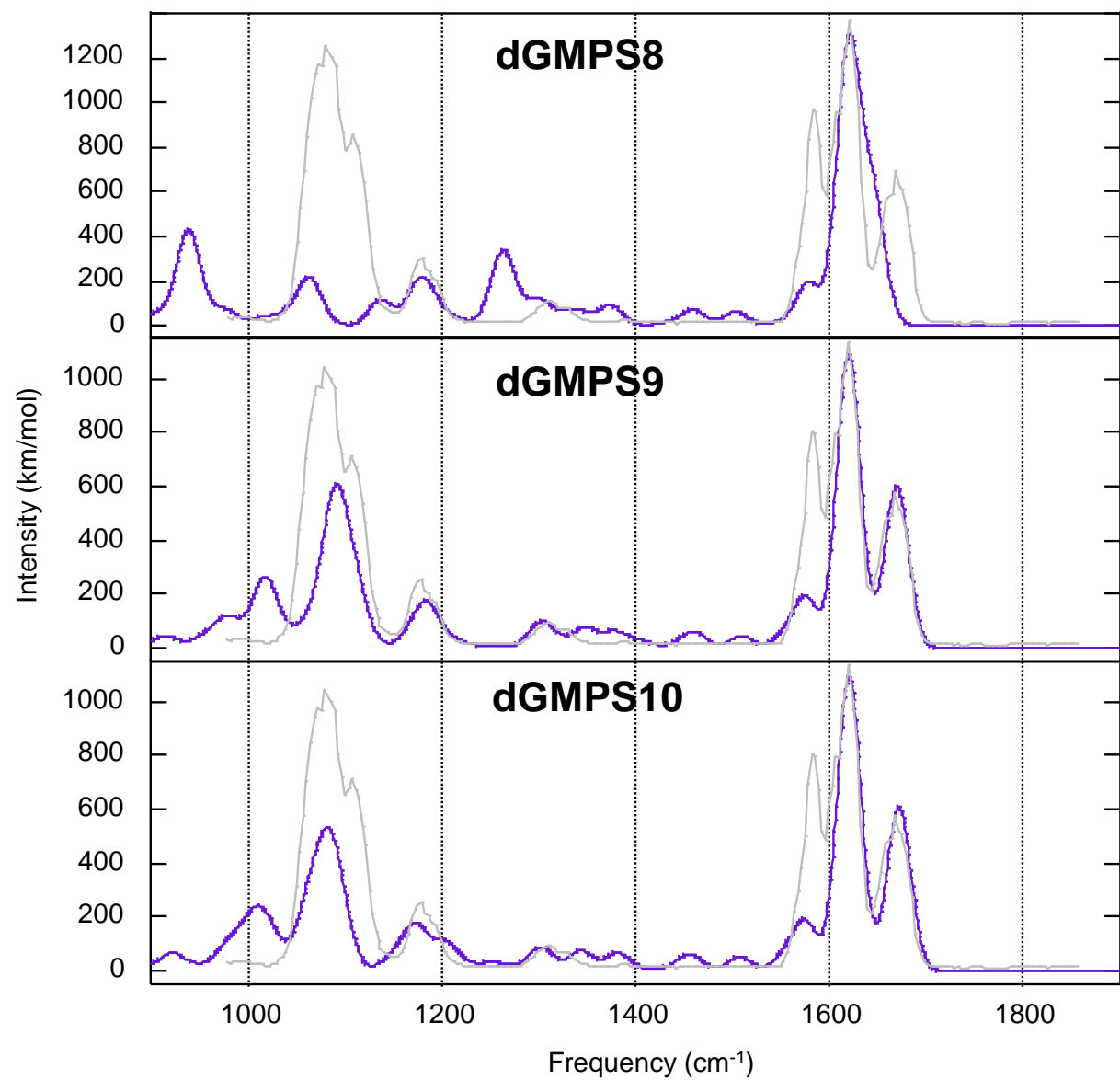
4S. DFT-computed IR absorption spectra for the $[\text{Pb}(\text{dGMP})\text{-H}]^+$ structures. The experimental IRMPD spectrum is overlayed in grey.











5S. Evolution of $[\text{Pb}(\text{dGMP})\text{-H}]^+$ drift time as a function of $1/E$, E the electric field applied across the mobility tube. Inset shows an arrival time distribution at $E = 700\text{V/m}$ (blue) overlaid with the predicted distribution (red) for a single conformation by the same experimental conditions. The predicted distribution for CCS 10% higher (dashed green) is well separated, showing that only one family of conformations is observed experimentally. The CCS of the $[\text{Pb}(\text{dGMP})\text{-H}]^+$ complex is determined from the slope of the line as 99.6\AA^2 .

